International Journal of
INTELLIGENT SYSTEMS AND APPLICATIONS IN ENGINEERING
ISSN:2147-6799 www.ijisae.org Original Research Paper

A Reliable Tool Based on the Fuzzy Logic Control Method Applying to the DC/DC Boost Converter of Off-Grid Photovoltaic to Track the Maximum Power Point

Pham Hong Thanh[1], Le Van Dai[2*]

Submitted: 08/05/2023 **Revised**: 13/07/2023 **Accepted**: 07/08/2023

Abstract: Solar energy performs an important role in electric energy based on renewable energy generation systems when referring to clear energy. Systems for harvesting renewable energy frequently use DC/DC converters, especially solar photovoltaic systems. The DC/DC boost converter has been used for converting the output voltage from the solar PV system to the required voltage rating of the utility grid under the disturbance in the photovoltaic temperature and irradiation level. Because of that, a new maximum power point tracking based on the fuzzy logic controller (MPPT-FLC) algorithm applying the DC/DC boost converter is developed. The proposed approach aims toward improving the PV system's performance and tracking effectiveness. This aim can be achieved by adjusting the DC/DC boost converter's duty cycle to ensure that the PV system operates close to its MPP under varying environmental conditions. The effectiveness of the proposed method is verified in the off-grid PV system under conditions of the change of irradiation and temperature, and the comparison of between the proposed method, the incremental conductance (INC), perturb and observe (P&O), and modified P&O methods is also made. The obtained simulation results show that the MPPT capability significantly improved and achieved the highest MPPT efficiency of 99.999% and an average efficiency of 99.98% in total when applying the proposed method.

Keywords: *DC-DC converter, fuzzy logic, incremental conductance, perturb and observe, solar photovoltaic, maximum power point*

1. Introduction

Researchers worldwide have been trying to find alternative solutions to traditional energy sources using energy from dispersed sources to reduce costs, pollution, and other environmental issues caused by fossil fuel-powered generators for the past few decades. Solar photovoltaic (PV) has emerged as a leading option to replace costly and environmentally damaging conventional power sources. Solar PV is preferred because of its safety, long lifespan, low maintenance, and cost-effectiveness. The widespread availability and extensive utilization of solar PV systems, both in independent setups and grid-tied configurations, underscore the growing popularity and practicality of solar energy as a sustainable solution for power generation.

The most basic independent solar power system includes a module or a string of solar panels combined with a DC/DC converter that provides the load's power. The converter may increase or decrease the panels' voltage based on the system's characteristics. The independent solar energy system surveyed in this article is presented in Fig. 1.

[1] *Institute of Engineering and Technology, Thu Dau Mot University, Binh Duong Province, Vietnam.*
ORCID ID: 0009-0001-3463-7099
[2] *Electric Power System Research Group, Faculty of Electrical Engineering Technology, Industrial University of Ho Chi Minh City, Ho Chi Minh City, Vietnam.*
ORCID ID: 0000-000 1-9312-0025
** Corresponding Author Email: levandai@iuh.edu.vn*

Extensive research on the maximum power point tracking (MPPT) methods has been conducted over the past decade, focusing on different techniques' speed, accuracy, and complexity. These requirements, such as the physical information needed from the PV modules, can impact computing power and efficiency. In recent years, there has been a surge in research on MPPT methods, as evidenced by the increasing number of studies published in this field. This research has led to the development of new and improved MPPT techniques, improving PV systems' efficiency and making them more reliable and cost-effective.

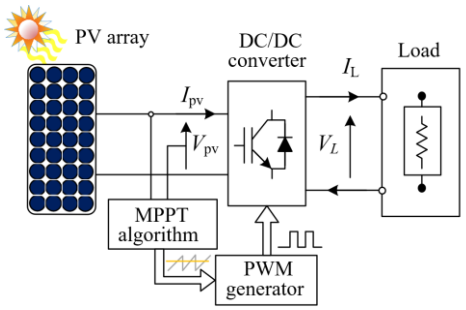

Fig. 1. The off-grid PV system

In [1], the authors presented the modeling, simulating MPPT methods using the P&O and the INC for the independent PV systems. The P&O and INC algorithms were explained and tested in detail. They compared the results under various solar radiation conditions with different working temperatures. In addition, the study also compared the effect when the system applied MPPT as the

P&O and INC with a fixed duty value of 0.35% and without MPPT. In [2], authors have introduced an MPPT method with high accuracy and the shortest response time, and this method is compared to the P&O, INC, and fuzzy logic controller (FLC). In addition to describing in detail the proposed MPPT method, the paper also presents comparative results showing the outstanding advantages of the proposed method: faster than four times compared to P&O, five times compared to INC, and about 28% compared to FLC. However, the suggested approach based on FLC also utilizes extra sensors to detect solar radiation and the temperature of the PV module in addition to the voltage and current sensors for the PV, which increases because of these sensors cost. The authors compared the P&O and hill-climbing (H-C) three-point MPPT methods in their study. Performing MPPT algorithms under varying conditions for a 10.2 kW PV system between P&O, INC, extremum seeking control (ESC), and FLC [3] showed that FLC was the best algorithm compared with others in all cases. However, this study only evaluates the cases of radiation intensity changes rapidly but has not done for the cases of slow change and evaluates the effectiveness of MPPT. In [4], the authors have explained in detail the differences between the conventional two-point P&O algorithm and the three-point P&O algorithm. The authors were concerned with performance criteria such as efficiency, the PV operating voltage, and MPP tracking accuracy under condiring the changes in ambient temperature and radiation intensity.

Recently, the comparison between methods has also been introduced, such as the P&O, INC and P&O-backstepping controller (BSC) [5], artificial neural network (ANN)-integral sliding mode controller (ISMC) [6], ANN-BSC and ANN- integral feedback linearization controller (IFLC) [7]. The ISMC, IFLC, and BSC could control non-linear systems such as PV with fast responses to changes in input parameters and it also demonstrated resilience to system parameter variations or sensor errors. The application of ANN-IFLC in MPPT for the PV systems under different changing conditions gave better results than the algorithms in the study. The authors [8] presented a study on the fixed step size INC-MPPT and the adaptive step size Neuro-Fuzzy INC-MPPT. The results showed that the Neuro-Fuzzy-INC algorithm outperformed the IC-MPPT. The suggested method can improve the output power and significantly reduce the power losses through the simulation comparison of the system using MATLAB/Simulink.

The studies mentioned above have highlighted numerous outstanding advantages of FLC and the weaknesses of conventional P&O, such as MPPT techniques that observe the increasing conduction correlation between the PV sources and loads. Some research has shown that the effectiveness of many MPPT techniques can be improved by applying different methods to enhance their performance. Furthermore, studies have shown that hybrid approaches such as ANFIS produce better results than their original counterparts.

This paper introduces a new tool based on the fuzzy logic control method to track the MPP applying the DC/DC boost converter of off-grid photovoltaic. The following brief summary lists the primary particular contributions:

(*i*) Building MPPT-FLC algorithm by calculating the grad slope from the voltage and current at the working point on the P-V cure of PV, in which the voltage and current signals are processed through the zero-order hold (ZOH) stage with the purpose of increasing control system stability;

(*ii*) Testing for the working mode of the PV module under the conditions of fast and slow irradiation change from 0 to 1000 W/m^2 and the sine change of temperature from 20 to 50^{o}C, it is the same to change almost randomly and continuously, closing to actual operating conditions;

(*iii*) Applying SimCoupler to simulate the tested system via time domain by combining PSIM and MATLAB.

The next parts of the paper are structured as follows: The basic theory of the PV module model, followed by the explanation of the structure and operation of the boost converter presented in Section 2. In section 3, an overview of the MPPT techniques for the PV system is provided, and details of the MPPT techniques based on fuzzy logic are given. Simulation results and discussions are presented, comparing them with other traditional MPPT methods such as P&O and INC in section 4. Finally, a conclusion is reached in the paper.

2. Materials and Method

2.1. Solar photovoltaic model

Solar modules typically consist of multiple solar cells connected in series or parallel to achieve a higher output power suitable for the application requirements. The PV cell is simplified by an equivalent circuit, as shown in Fig. 2 [9-11]. It consists of a current source, a shunt diode, a parallel resistor and a series resistor.

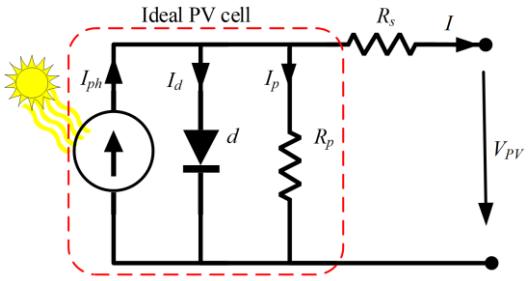

Fig. 2. Solar module circuit

The diode PV cell has the following characteristics [9-11]:

$$I = I_{ph} - I_d - \frac{V_{PV} - I.R_s}{R_p} \quad (1)$$

where:

$$I_d = I_0 \left(e^{\frac{q(V_{PV} + R_s I)}{nkT_a}} - 1 \right) \quad (2)$$

in which I, I_d, I_p, and I_{ph} are the series resistor, the diode saturation, parallel resistor, photovoltaic currents; q is elementary charge and can be chosen 1.60217646.10-19 C for this paper; n is the diode ideality factor; k is the Boltzmann constant and can be chosen 1.3806503.10-23J/K for this paper; Ta is the ambient temperature; V_{PV} is the terminal voltage of the PV cell; R_p and R_s are the parallel and series resistors.

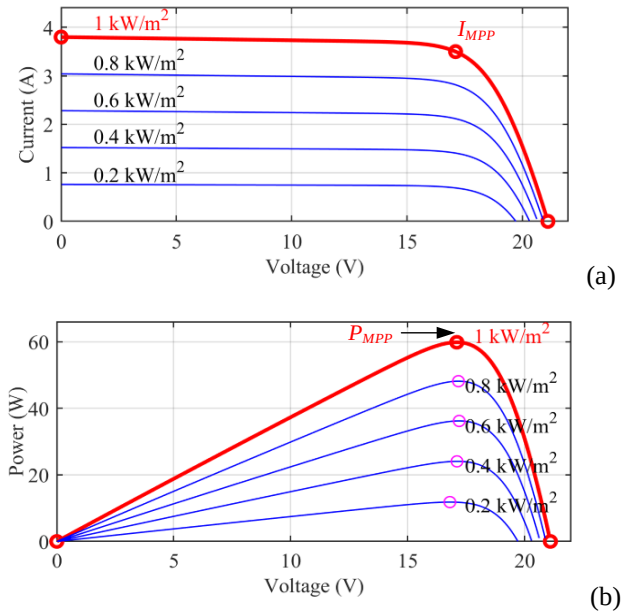

Fig. 3. The characteristic of the PV module at constant temperature and variable irradiant: (a) *I-V* curve and (b) *P-V* curve

The operating characteristics of a PV module depend on the solar irradiance and module temperature conditions. Fig. 3 shows the characteristics of the PV module at constant temperature, a variable radiation performed in the *I-V* and *P-V* curves. The module will produce maximum power at a single operating point denoted by I_{MPP} and V_{MPP}. It is possible to calculate the MPP position based on the measured solar irradiance and module temperature from sensors for control purposes. To extract the maximum output power from the PV module, operating it at the MPP is necessary. The PV module's temperature and solar irradiation are the primary determinants of the MPP. The MPP of the system is constantly changing as these parameters change over time, sometimes randomly due to the environment [11].

2.2. DC/DC boost converter

PV solar technology is characterized by the conversion of sunlight into direct current (DC) electrical energy. Despite persistent research and advancements in photovoltaic panel technology, the efficiency of converting sunlight into electricity remains comparatively low. Further research and development efforts are required to enhance the overall conversion efficiency and optimize the performance of the PV systems. The highest conversion efficiency is only around 20% or slightly higher. Therefore, optimizing the PV system efficiency is always essential [12]. The power semiconductor switch of the power converter must be controlled so that the maximum power is extracted from the PV system to supply the load. Some techniques and strategies to achieve this control are known as MPPT. The schematic diagram of the boost circuit is shown in Fig. 4. The periodic switching of the power semiconductor switch *SW* is the reason why the output voltage exceeds the input voltage. The inductor in the circuit acts as an energy storage device, which releases energy from the magnetic field during the operation of the circuit [13].

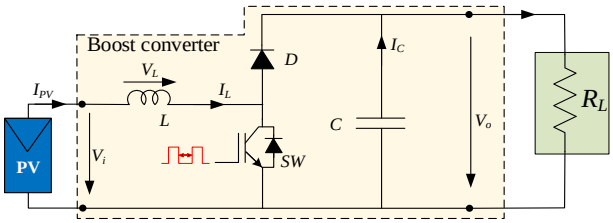

Fig. 4. DC/DC boost converter

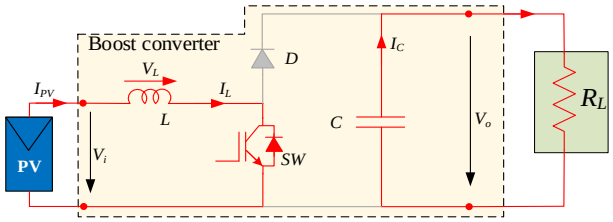

Fig. 5. DC/DC boost converter in mode 1

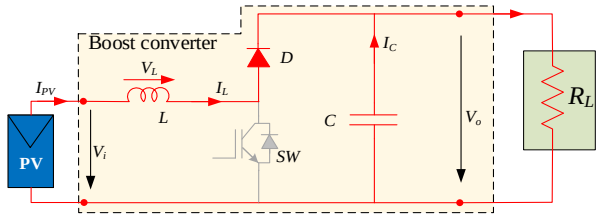

Fig. 6. DC/DC boost converter in mode 2

Depending on the *SW*'s state, the boost converter circuit will operate in one of two modes.

For mode 1, as shown in Fig. 5, when the switch *SW* is closed during time $t = t_{ON}$. The current entering the boost circuit increases and passes through the inductor *L*.

For mode 2, as shown in Fig. 6, when the *SW* opens during time $t = t_{OFF}$. The current flows through *L*, *C*, diode (*D*), and the load. Until the next cycle starts, the current in *L* decreases. The energy stored in *L* passes through the load in mode 2 [14].

Currently, discontinuous conduction mode (DCM) and continuous conduction mode (CCM) are widely used models for DC/DC step-up inverters, but they depend on several factors. However, CCM can benefit DCM by using a more comprehensive operating range, improved output voltage control, and reduced peak current stress. Additionally, CCM benefits from the availability of numerous components and reference designs due to its maturity as a technology. Consequently, this study will select parameters for the DC/DC boost inverter to operate in CCM. The operation and waveforms are in Fig. 7.

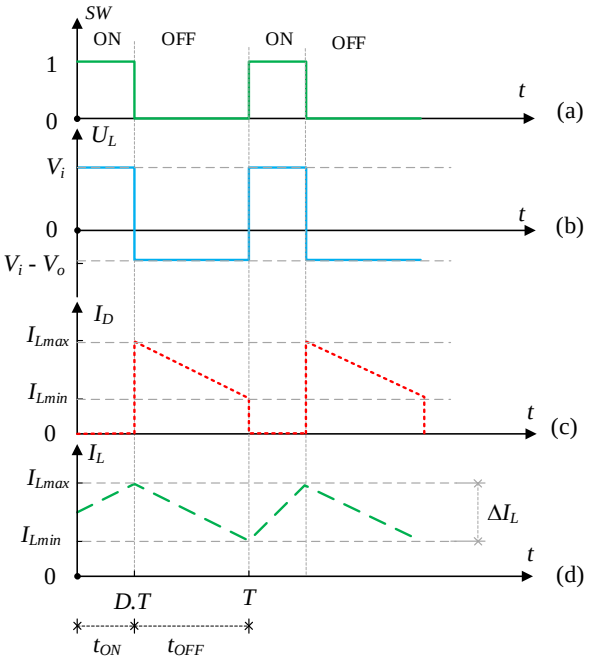

Fig.7. CCM waveforms of DC/DC boost converter: (a) the *SW* operates; (b) Inductor voltage; (c) Diode current; (d) Inductor current

With the ideal converter circuit, we have the following equations [15]:

$$P_{out} = P_{in} = P_{pv} \tag{3}$$

$$\frac{V_{out}}{V_{pv}} = \frac{I_{pv}}{I_{out}} = \frac{1}{1-D} \tag{4}$$

$$V_{out}.I_{out} = V_{pv}.I_{pv} \tag{5}$$

The equivalent resistance of the load at the side of the DC/DC boost converter is calculated as follows:

$$R_{eq} = R_L(1-D)^2 \tag{6}$$

where *D* is the duty cycle, and R_L is the load resistance. The equivalent resistance depends on *D*. Therefore, to extract and harvest the maximum power from the PV source, a control monitoring system is required to regulate the values of *D*. This control system is commonly referred to as an MPPT controller [14]. Several solutions are available to implement MPPT, which will be presented in the next section of this article.

3. Mppt Algorithms

The DC/DC converter is critical in driving the PV array at the MPP when the sun's insolation fluctuates. According to the maximum power transfer theorem, the load will get its peak power if its impedance is equal to the complex conjugate of the supply system's internal impedance [16, 17]. The DC/DC converter is essential for driving the PV cluster to the MPP when sunlight varies. According to the maximum power transfer theory, the load will receive maximum power if its impedance equals the complex conjugate of the supply system's impedance.

3.1. Perturb and Observe Algorithm

The P&O-MPPT algorithm provides a straightforward and efficient approach to monitoring a PV system's MPP while ensuring originality. The MPP designates the moment when the PV system generates the utmost power capacity. The algorithm commences by initializing the PV system's operating point at a random value [18-20]. Following this, it introduces a minor adjustment to the operational point. Subsequently, the algorithm gauges the ensuing alteration in power output. If power output experiences an upsurge, the algorithm progresses in the direction of modification. Conversely, if power output declines, the algorithm shifts against the initial adjustment's direction.

The P&O algorithm's functionality is grounded in the cyclic modification of the PV system's operational point and the subsequent assessment of power output changes. The algorithm systematically advances towards augmented power output until the MPP is attained. Nonetheless, the concurrence to the MPP may exhibit sluggishness, particularly in circumstances characterized by rapid MPP fluctuations. The rate of convergence for the P&O algorithm correlates with the magnitude of the adjustment. Larger adjustments expedite convergence but concurrently elevate the risk of overshooting the MPP [1, 19]. The flow diagram appears in Fig. 8.

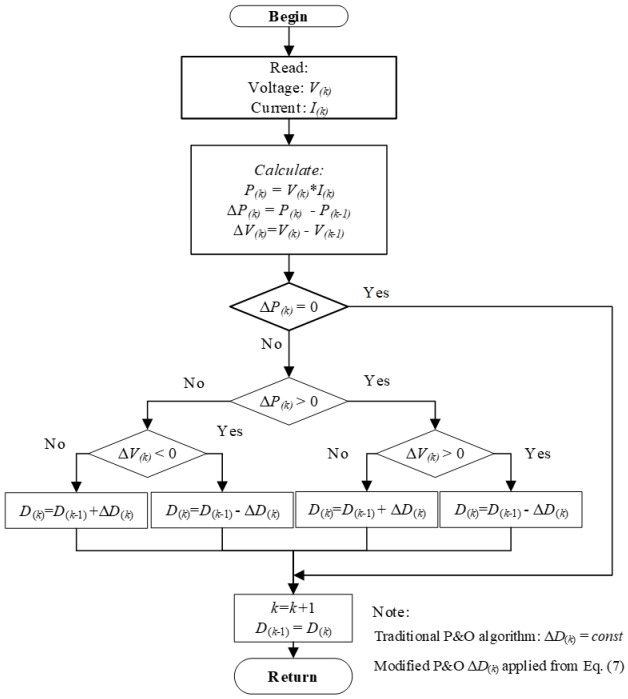

Fig .8. Flow diagram of P&O algorithm

The modified P&O algorithm [20] presents a variable duty, and the k^{th} duty can be determined as follows:

$$\Delta D_{(k)} = M \left| \frac{\Delta P_{(k)}}{\Delta V_{(k)}} \right| \tag{7}$$

where $\Delta D_{(k)}$ can changed to bring the system quickly to MPP and reduce fluctuations when the system is working at MPP, M is a constant that depends on the working system and needs to be calibrated depending on the system parameters, and $\Delta P_{(k)}$ and $\Delta V_{(k)}$ are the power and voltage change at the k^{th} of PV module and they can be determined as follows, respectively [21]:

$$\Delta P_{(k)} = V_{(k)} I_{(k)} - V_{(k-1)} I_{(k-1)} \tag{8}$$

$$\Delta V_{(k)} = V_{(k)} - V_{(k-1)} \tag{9}$$

where $V_{(k)}$ and $I_{(k)}$ are the voltage and current at the k^{th} step, respectively, and $V_{(k-1)}$ and $I_{(k-1)}$ are the voltage and current at the $(k\text{-}1)^{\text{th}}$ step, respectively.

3.2. Incremental Conductance Algorithm

The MPPT-INC algorithm, recognized for its simplicity and precision over the widely used P&O technique, optimizes power extraction from photovoltaic systems. Operating through power converters, it adjusts the duty cycle (D) based on voltage and current conditions for superior efficiency. During implementation, a regulated step size is employed to fine-tune duty cycle changes. A small step size results in gradual power vacillations and sluggish responses, while a larger step size can induce excessive oscillations [22-24]. The central challenge involves striking a balance between swift responses and steady-state accuracy, as fixed step sizes typically struggle with this equilibrium. Despite the algorithm's success in tracking accuracy, its performance in the face of external disturbances remains uncertain due to the absence of testing in that context. A viable solution entails incorporating a variable step size, which diminishes as the algorithm approaches the optimal power point. This dynamic adjustment facilitates both rapid responses and stable performance. Actually, since a variable step estimate performs smaller increases as long as the calculation approaches the specified working control point, which is the case with most typical MPPT calculations, both quick elements and steady-state exactness cannot be achieved at the same time [25, 26]. The flow diagram is presented in Fig. 9.

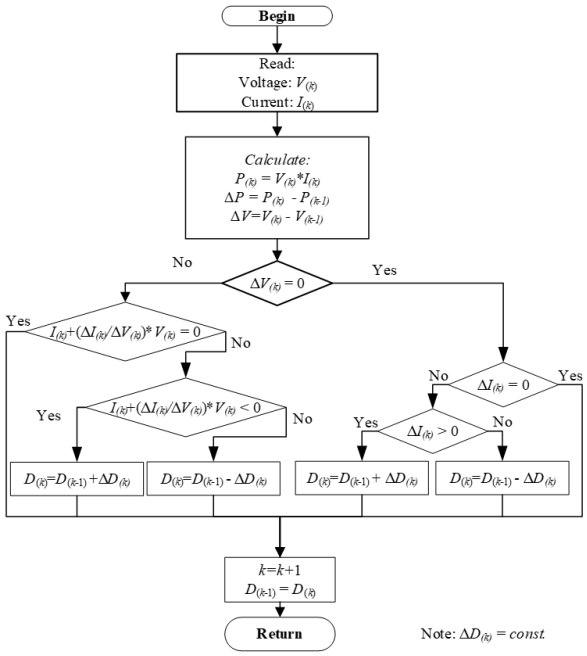

Fig.9. Flow diagram of INC algorithm

3.3. Proposed algorithm

The MPPT-FLC algorithm is an intelligent approach aimed at tracking the optimal operating power point in PV systems [27]. Unlike relying solely on the system's mathematical model, FLC draws inspiration from human experience. By mimicking human decision-making processes, FLC enhances its ability to adapt and optimize power extraction effectively [28]. Therefore, the suggested tracking method is formulated using a gradual and adaptive exploration approach.

Without the approach of using V and I inputs of PV module in literature [28], this study proposes to use the grad slope value of the operation characteristic P-V curve as shown in Fig. 10 and its variation to determine the change duty at MPPT steps for FLC. The grad slope is determined as follows [21]:

$$grad\theta_{(k)} = \frac{\Delta P_{(k)}}{\Delta V_{(k)}} \tag{10}$$

Based on the fact that the PV array's *P-V* slope is zero at the MPP, Fig. 10 provides three circumstances that may be characterized as follows:

i) $grad\theta_{(k)} > 0$: on the left of MPP, the voltage and power increase in this case.

ii) $grad\theta_{(k)} < 0$: on the right of MPP, in this case, the power decreases and the voltage increases.

iii) $grad\theta_{(k)} = 0$: at MPP.

The MPPT-FLC structure, as shown in Fig. 11, includes the fuzzification, inference engine, and defuzzification blocks**.** The first block is the fuzzification block containing two input variables of the error $E_{(k)}$ and changes in error $\Delta E_{(k)}$ at the k^{th} operation value. These variables are defined by using Eqs. (11) and (12) respectively. The error $E_{(k)}$ is assigned to the $grad\theta_{(k)}$ of k^{th} point *P-V* characteristic of PV. The instantaneous power of the PV array is denoted as $P_{pv(k)}$, and the DC link voltage is represented as $V_{(k)}$. When $E_{(k)}$ is greater than zero, the system is heading towards the MPP; when $E_{(k)}$ equals zero, it's operating at the MPP; and when $E_{(k)}$ is less than zero, it moves away from the MPP.

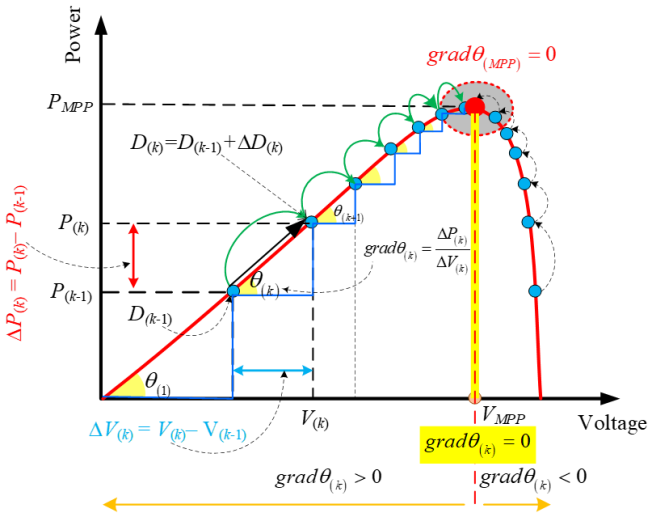

Fig. 10. MPPT operation based on *P-V* characteristic curve

$$E_{(k)} = grad\theta_{(k)} = \frac{\Delta P_{(k)}}{\Delta V_{(k)}} \tag{11}$$

$$\Delta E_{(k)} = E_{(k)} - E_{(k-1)} = \left(grad\theta_{(k)} - grad\theta_{(k-1)}\right) \tag{12}$$

The second functional block entails the execution of membership rules known as an "inference engine", where the user's basic logic is decoded. Table 1 displays a comprehensive set of fuzzy linguistic rules comprised of 25 distinct situations, and the notations are denoted the negative big (NB), negative medium (NM), negative small (NS), zero (Z), positive small (PS), positive medium (PM), and positive large (PB) [29, 30]. These rules are set on the IF-THEN statement, as explained in the following examples:

IF [($E_{(k)}$=NS) and ($\Delta E_{(k)}$=PS)] THEN [$\Delta D_{(k)}$=PS]

IF [($E_{(k)}$=PS) and ($\Delta E_{(k)}$=Z)] THEN [$\Delta D_{(k)}$=NS]

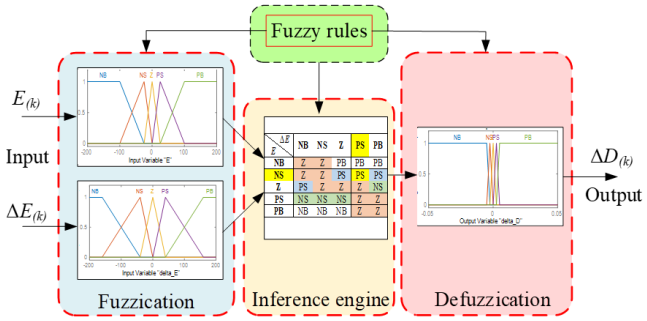

Fig. 11. Fuzzy logic control structure block

Table 1: Rules for the FLC

$E_{(k)}$ \ $\Delta E_{(k)}$	**NB**	**NS**	**Z**	**PS**	**PB**
NB	Z	Z	PB	PB	PB
NS	Z	Z	PS	PS	PS
Z	PS	Z	Z	Z	NS
PS	NS	NS	NS	Z	Z
PB	NB	NB	NB	Z	Z

The third functional component, known as "defuzzification", is responsible for transforming the inference engine's verbal instructions into numerical crisp values. After "defuzzification," which is accomplished using the center of gravity technique. The fuzzy system's output may be described as follows [31]:

$$\Delta D_{(k)} = \frac{\sum_{i=1}^{n}\left[\Delta D_i \times \mu\left(\Delta D_i\right)\right]}{\sum_{i=1}^{n}\Delta D_i} \tag{13}$$

where n is the number of IF-THEN rulers and $\mu(\Delta D_i)$ presents the minimum membership of the i^{th} rule.

The fuzzy toolbox in MATLAB software was used to create the input and output membership functions [32, 33]. These functions are then displayed in Fig. 12 (a) and 3-D control surface in Fig. 12 (b).

4. Simulation Results

4.1. System and elements set up

Fig. 13 depicts the simulated off-grid PV system. In this figure, it has two blocks. The first one is the proposed MPPT control one is established and second on is the

PSIM_Coupler is established PSIM. This simulated system has two inputs, which are voltage (VA) and current (IA) of PV from the power circuit in PSIM transferred to MATLAB by PSIM_Coupler block. The output of the MPPT controller is the PWM value returned to the PSIM to control the boost converter.

In this paper, the *SW* frequency is chosen f_{SW} = 20kHz. L = 1.5mH, C_i = C_o = 150µF, time step is 1x10^{-6}s. Because R_{eq} of Load is calculated by (6), the D is between 0÷1, so the value of R_{load} will be chosen to satisfy the condition larger than the R_{MPP} of the PV module at the lowest operation condition (100W/m^2) is about 40Ω. Thus, the R_{load} in this survey is 50Ω. In this study, the ZOH function block for each voltage and current signal of PV is used to improve the stability and performance of control systems.

The specific PV module parameters employed in the experimental model are detailed in Table 2.

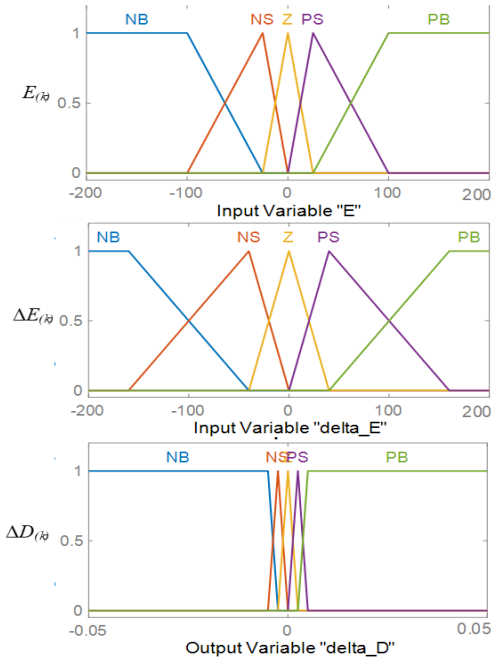

(a)

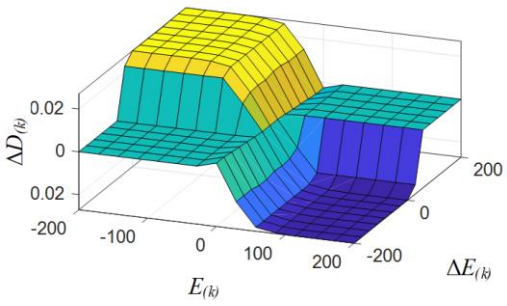

(b)

Fig. 12. The fuzzy processing procedure: (a) Relationship function;
(b) 3-D control surface viewer

The efficiency analysis in response to four MPPT algorithms, including P&O [24], INC [24], and modified P&O [20], and this proposed method is demonstrated under considering the model changes in radiation conditions and working temperature, as shown in Fig. 14. To reduce the oscillation at MPP, the ΔD of P&O and INC will be chosen and fixed at 0.3%. In contrast, the modified P&O and the proposed method will have flexible ΔD based on the proposed algorithm.

Table 2. Electrical characteristics of the PV module

Parameters	**Values**
The maximum power (P_{max}) at MPP	60 W
The voltage at P_{max} (V_{mpp})	17.0 V
The current at P_{max} (I_{mpp})	3.53 A
The open circuit voltage (V_{oc})	21.1 V
The short circuit current (I_{sc})	3.8 A
The temperature coefficient of V_{oc}	-(80 ± 10) % V/^{0}C
The temperature coefficient of I_{sc}	-(0.065 ± 0.015) % V/^{0}C
The temperature coefficient of power	-(0.5 ± 0.05) % V/^{0}C
The nominal operating cell temperature	47 ± 2 ^{0}C
The operating temperature	25 ^{0}C

4.2. Performance evaluation

The effectiveness of the proposed MPPT-FLC and three other algorithms is measured by MPPT efficiency. The instantaneous MPPT efficiency was calculated according to the following equation:

$$\eta_{MPPT} = \frac{P_{MPPT}(t)}{P_{MPP^*}(t)} \times 100\% \quad (14)$$

The average MPPT efficiency is given by:

$$\eta_{MPPT(avg)} = \frac{\int P_{MPPT}(t)dt}{\int P_{MPP^*}(t)dt} \times 100\% \quad (15)$$

where, P_{MPP^*} is the maximum power of PV can be archived by signal in the PV module of simulation. Besides, it is also the target of the MPPT algorithm. On the other hand, P_{MPPT} is the power of PV module by using MPPT algorithms to harvest the power. This value depends on the ability of the algorithm to track the MPP of PV at any time with its irradiation and temperature.

In this study, we aim to compare the performance criteria of the algorithm, so we will focus on presenting the power results obtained from the PV module and MPPT time for evaluation. Two cases of system change due to environmental influences will be presented as follows:

Case 1: The performance of the proposed control stratagem is verified through the varying irradiation while keeping constant temperature at 25 ºC. In this case, the input of PV is irradiation varied, as shown in Fig. 14 (a). In this case, the system response for the four methods is shown in Fig. 15. Observing these results shows that the FLC algorithm exhibits an exceptionally fast MPPT time of approximately 0.02 seconds, P&O and INC to need 0.06 seconds to reach the MPP from starting. The modified P&O is faster and needs almost FLC times as 0.02 seconds. Furthermore, the comparisons of V_{PV}, V_{out}, I_{PV}, I_{out}, MPPT efficiency and duty cycle are also present in Fig. 15 (b)-(g). From Fig. 15 (a) and (f), we can see that the PV's power and MPPT efficiency of the proposed FLC have the largest values in both indexes (the PV's power always reaches almost to the P_{MPP*} and the MPPT efficiency is almost 99.999%~100%) compared with surveyed algorithms. The next good algorithm is modified P&O [20]. Although it has drifted in some cases, the overall MPPT efficiency is still so good, with over 99.98% as Fig. 15 (f). The duty cycles of all surveyed algorithms are the same sharp as in Fig. 15 (g), but the proposed FLC and modified P&O have less oscillation in stable conditions and are more well done in transient times. But the modified P&O also had some drift durations. So, FLC is the most effective MPPT algorithm for control to collect more power and better immediate efficiency, and also the average one for all time.

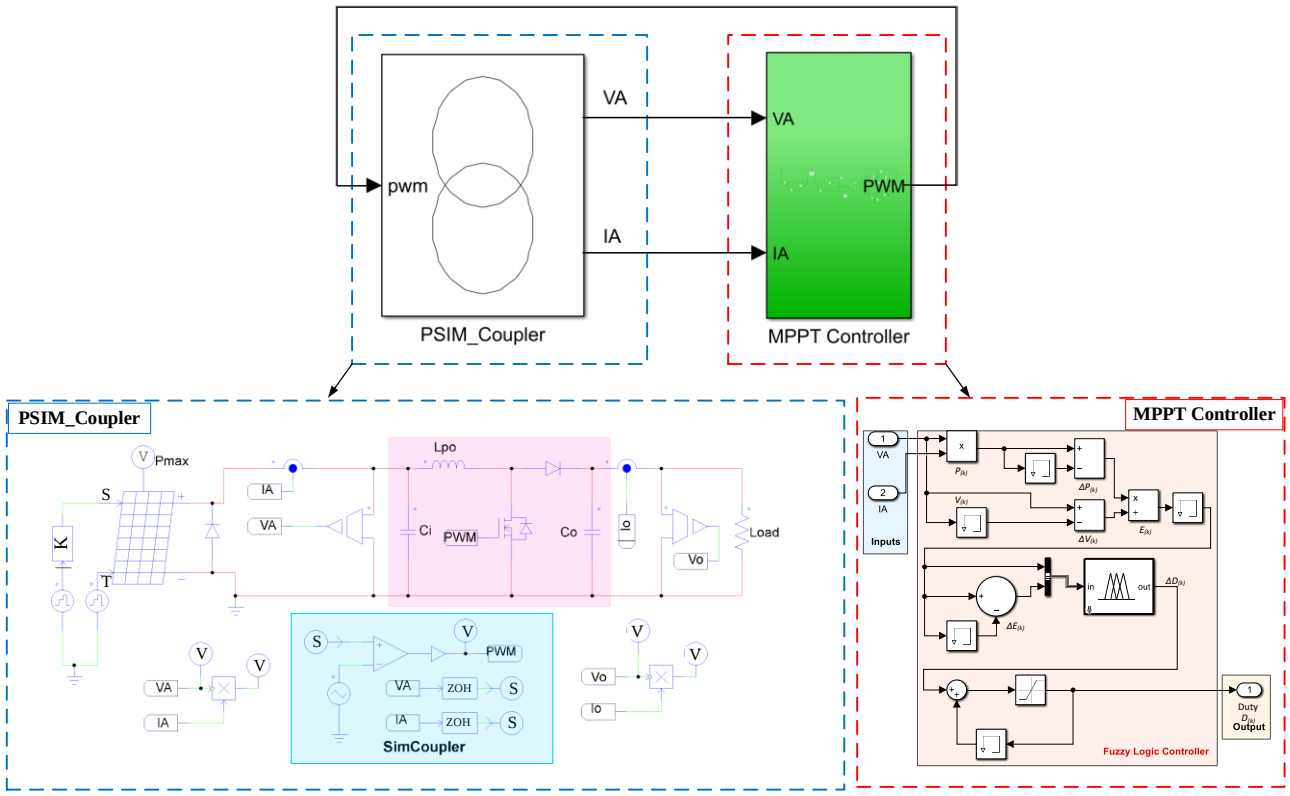

Fig. 13. The simulated off-grid PV system

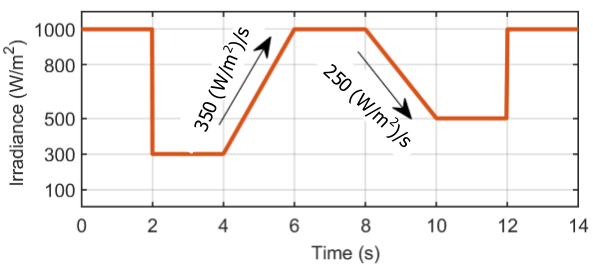

(a)

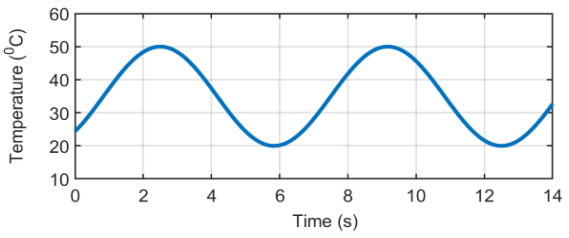

(b)

Fig. 14. The simulation scenario: (a) the varying irradiation, (b) varying temperature

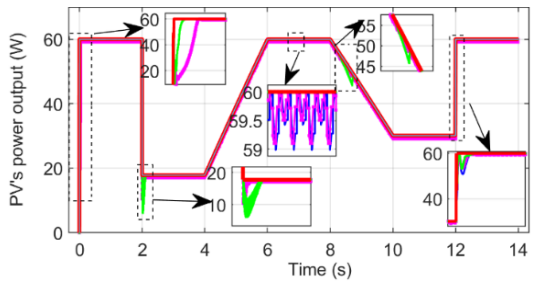

(a)

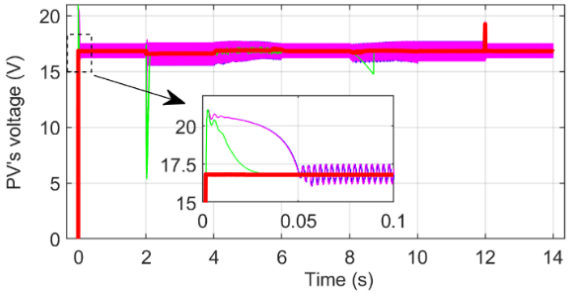

(b)

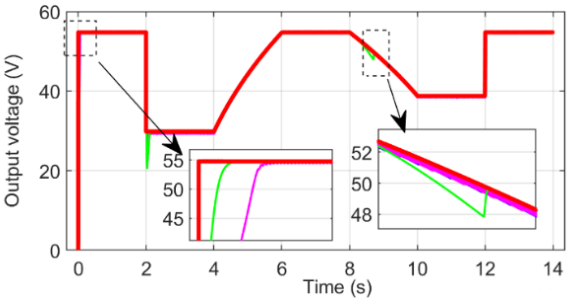

(c)

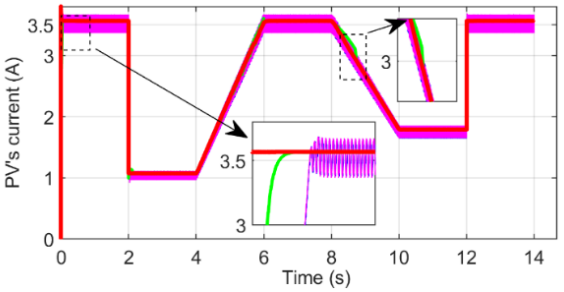

(d)

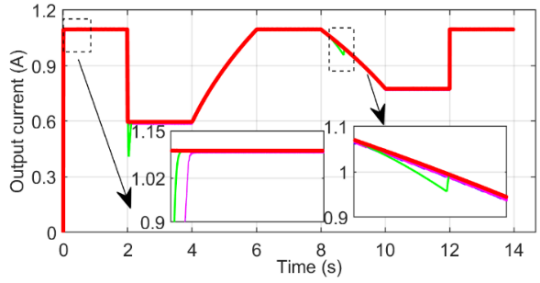

(e)

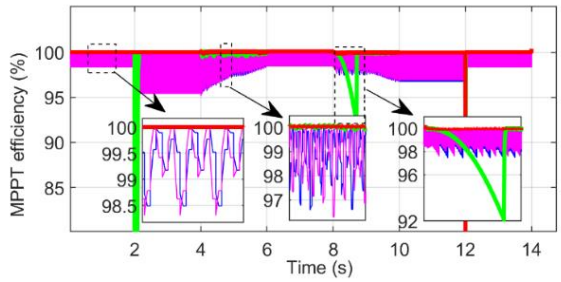

(f)

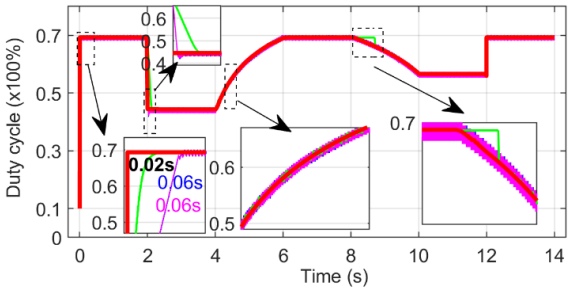

(g)

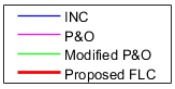

Fig. 15. The response in Case 1: (a) PV's power output, (b) PV's voltage output (V_{pv}), (c) Output voltage (V_o), (d) PV's current (I_{pv}), (e) Output current (I_o), (f) MPPT efficiency, (g) Duty cycle

Case 2: The performance of the proposed control stratagem is verified through variations in both temperature and irradiation. In this case, the varying inputs of PV are shown as shown in Fig. 14. The system response for four methods in this case is shown in Fig. 16. Observing these obtained results, the parameters of radiation intensity and operating temperature directly affect the P_{MPP*} of PV to test the stability of the control algorithm under different conditions.

The power output of the PV module represented in Fig. 16 (a) demonstrates the constrained performance of conventional P&O and INC algorithms under rapidly changing environmental conditions, specifically at elevated temperatures affecting the MPPT control. The sluggish response time and oscillations observed during system control contribute to these limitations. The tracking time in Case 2 is the same as in Case 1, which demonstrates the effectiveness of the proposed MPPT algorithms. The FLC algorithm is particularly effective, achieving the best results. Furthermore, the modified P&O solution, based on the traditional P&O technique, also displays commendable results while offering the advantage of simpler handling when compared to FLC. This aspect also warrants careful consideration. Another more, the comparisons of V_{PV}, V_{out}, I_{PV}, I_{out} and the MPPT efficiency are also present in the Fig. 16 (b-f).

Observing the obtained results in two study cases shows that

the duty cycle (%) changes rapidly according to the P_{MPP} parameter of PV when applying the proposed method. This duty cycle oscillates at a fixed value initially set at 0.3% when applying the P&O and INC. For the modified P&O. In addition, in order to quickly response in cases where P_{MPP} changes suddenly, the system continuously changes, leading to drift or high fluctuations due to the setting of parameter M from Eq. (7).

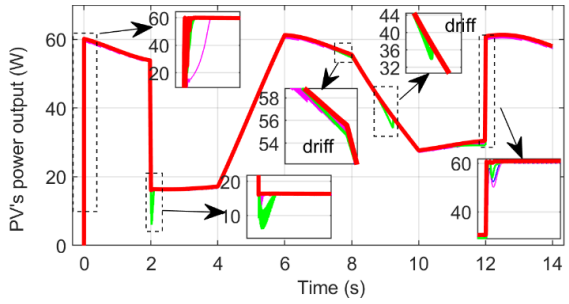

(a)

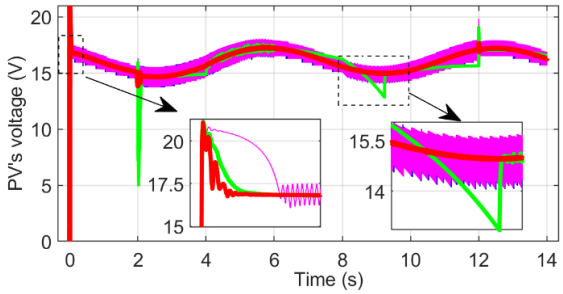

(b)

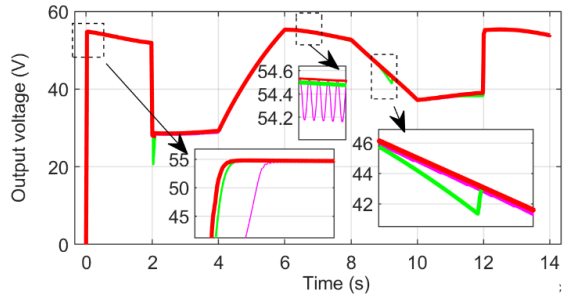

(c)

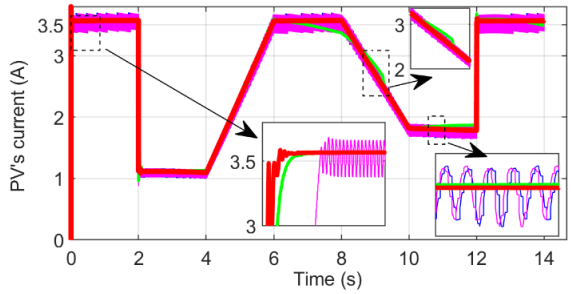

(d)

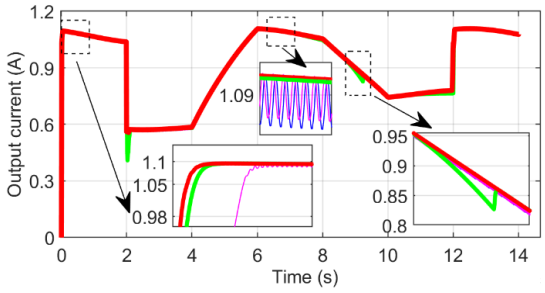

(e)

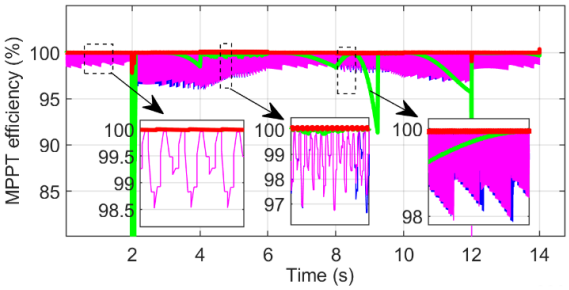

(f)

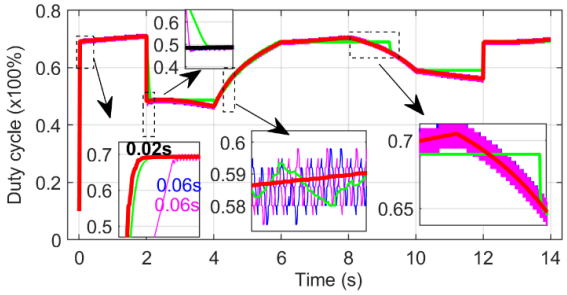

(g)

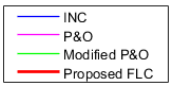

Fig. 16. The response in Case 2: (a) PV's power output, (b) PV's voltage output (V_{pv}), (c) Output voltage (V_o), (d) PV's current (I_{pv}), (e) Output current (I_o), (f) MPPT efficiency, (g) Duty cycle

5. Conclusion

This paper describes a proposed FLC for the DC/DC boost converter of a stand-alone solar power system. The circuit dynamics are simulated using PSIM software, while the control logic is programmed using MATLAB software. The two software are integrated by the SimCoupler module to exploit their strengths. The solar panel system has a capacity of 60 Wp, and the boost converter operates at a switching frequency of f_{sw} = 20kHz. The FLC adjusts $\Delta D_{(k)}$ based on the $grad\theta_{(k)}$ value of the operational point on the *P-V* characteristic curve and its variation after each k^{th} period.

Furthermore, the ZOH step is a useful technique for increasing control system stability and performance. The performance of FLC is compared with conventional algorithms such as P&O, INC, and modified P&O with

adaptive $\Delta D_{(k)}$, showing that FLC achieves the highest efficiency of 99.999% and an average efficiency of 99.97% in the 14 seconds of two tested cases. This is more adaptive to climate change than conventional P&O, INC, and the modified P&O algorithm. The research results also demonstrate that the integration with MATLAB enables the application of advanced algorithms to PSIM for MPPT control of solar power systems.

Acknowledgments

This research is funded by Thu Dau Mot University, Binh Duong Province, Vietnam under grant number DT.21.1-068. We thank our colleagues from the Electric Power System Research Group, Industrial University of Ho Chi Minh City, Vietnam, and reviewers for comments that significantly improved the manuscript.

Author contributions

P.H. Thanh: Conceptualization, Methodology, Software, Field study, **L.V. Dai**: Data curation, Writing-Original draft preparation, Software, Validation., Field study. All authors have read and agreed to the published version of the manuscript.

Conflicts of interest

The authors declare no conflicts of interest.

References

[1] M. A. E. Eid, A. A. Elbaset, H. A. Ibrahim, and S. A. M. Abdelwahab, "Modelling, Simulation of MPPT Using Perturb and Observe and Incremental Conductance techniques For Stand-Alone PV Systems," *2019 21st International Middle East Power Systems Conference (MEPCON)*, pp. 429-434, 17-19 Dec. 2019 2019, doi: 10.1109/MEPCON47431.2019.9007962.

[2] U. Yilmaz, O. Turksoy, and A. Teke, "Improved MPPT method to increase accuracy and speed in photovoltaic systems under variable atmospheric conditions," *International Journal of Electrical Power & Energy Systems*, vol. 113, pp. 634-651, 2019, doi: 10.1016/j.ijepes.2019.05.074.

[3] B. K. Naick, T. K. Chatterjee, and K. Chatterjee, "Performance Analysis of Maximum Power Point Tracking Algorithms Under Varying Irradiation," *2017*, Photovoltaic system, MPPT algorithms, perturb and observe, incremental conductance, scalar gradient extremum seeking control, fuzzy logic controller. vol. 6, no. 1, p. 10, 2017-03-22 2017, doi: 10.14710/ijred.6.1.65-74.

[4] S. M. Fatemi, M. S. Shadlu, and A. Talebkhah, "Comparison of Three-Point P&O and Hill Climbing Methods for Maximum Power Point Tracking in PV Systems," *2019 10th International Power Electronics, Drive Systems and Technologies Conference (PEDSTC)*, pp. 764-768, 12-14 Feb. 2019 2019, doi: 10.1109/PEDSTC.2019.8697273.

[5] R. E. Idrissi, A. Abbou, M. Mokhlis, and M. Salimi, "A comparative study of MPPT control," *International Renewable Energy Congress (IREC)*, pp. 01-06, 20-22 March 2018 2018, doi: doi.org/10.1016/j.egypro.2018.11.201.

[6] C. Cheikh Ahmed, M. Cherkaoui, and M. Mokhlis, "MPPT Control for Photovoltaic System using hybrid method under variant weather condition," pp. 1-5, 2019, doi: 10.1109/WITS.2019.8723854.

[7] L. Bouselham, B. Hajji, and H. Hajji, "Comparative study of different MPPT methods for photovoltaic system," pp. 1-5, 2015, doi: 10.1109/IRSEC.2015.7455085.

[8] A. Harrag and S. Messalti, "IC-based variable step size neuro-fuzzy MPPT improving PV system performances," *Energy Procedia*, vol. 157, pp. 362-374, 2019, doi: doi.org/10.1016/j.egypro.2018.11.201.

[9] H. Bellia, R. Youcef, and M. Fatima, "A detailed modeling of photovoltaic module using MATLAB," *NRIAG Journal of Astronomy and Geophysics*, vol. 3, no. 1, pp. 53-61, 2019, doi: 10.1016/j.nrjag.2014.04.001.

[10] J. Gow and C. Manning, "Development of a photovoltaic array model for use in power-electronics simulation studies," *IEE Proceedings-Electric Power Applications*, vol. 146, no. 2, pp. 193-200, 1999, doi: 10.1049/ip-epa:19990116.

[11] M. A. Islam, A. Merabet, R. Beguenane, and H. Ibrahim, "Modeling solar photovoltaic cell and simulated performance analysis of a 250W PV module," *2013 IEEE Electrical Power & Energy Conference*, pp. 1-6, 21-23 Aug. 2013 2013, doi: 10.1109/EPEC.2013.6802959.

[12] M. Boztepe, F. Guinjoan, G. Velasco-Quesada, S. Silvestre, A. Chouder, and E. Karatepe, "Global MPPT Scheme for Photovoltaic String Inverters Based on Restricted Voltage Window Search Algorithm," *IEEE Transactions on Industrial Electronics*, vol. 61, no. 7, pp. 3302-3312, 2014, doi: 10.1109/TIE.2013.2281163.

[13] R. Ayop and C. W. Tan, "Design of boost converter based on maximum power point resistance for photovoltaic applications," *Solar Energy*, vol. 160, pp. 322-335, 2018, doi: 10.1016/j.solener.2017.12.016.

[14] F. Mumtaz, N. Zaihar Yahaya, S. Tanzim Meraj, B. Singh, R. Kannan, and O. Ibrahim, "Review on non-

isolated DC-DC converters and their control techniques for renewable energy applications," *Ain Shams Engineering Journal*, 2021, doi: 10.1016/j.asej.2021.03.022.

[15] S. Jana, N. Kumar, R. Mishra, D. Sen, and T. K. Saha, "Development and implementation of modified MPPT algorithm for boost converter-based PV system under input and load deviation," *International Transactions on Electrical Energy Systems*, vol. 30, no. 2, p. e12190, 2020, doi: doi.org/10.1002/2050-7038.12190.

[16] M. Lawan, A. Aboushady, and K. H. Ahmed, "Photovoltaic MPPT Techniques Comparative Review," *2020 9th International Conference on Renewable Energy Research and Application (ICRERA)*, pp. 344-351, 2020, doi: 10.1109/icrera49962.2020.9242855.

[17] S. Manna *et al.*, "Design and implementation of a new adaptive MPPT controller for solar PV systems," *Energy Reports*, vol. 9, pp. 1818-1829, 2023/12/01/ 2023, doi: 10.1016/j.egyr.2022.12.152.

[18] N. Femia, G. Petrone, G. Spagnuolo, and M. Vitelli, "Optimization of Perturb and Observe Maximum Power Point Tracking Method," *IEEE Transactions on Power Electronics*, vol. 20, no. 4, pp. 963-973, 2005, doi: 10.1109/tpel.2005.850975.

[19] F. Z. Hamidon, P. D. A. Aziz, and N. H. M. Yunus, "Photovoltaic array modelling with P&O MPPT algorithm in MATLAB," *2012 International Conference on Statistics in Science, Business and Engineering (ICSSBE)*, pp. 1-5, 10-12 Sept. 2012 2012, doi: 10.1109/ICSSBE.2012.6396616.

[20] J. Ahmed and Z. Salam, "An improved perturb and observe (P&O) maximum power point tracking (MPPT) algorithm for higher efficiency," *Applied Energy*, vol. 150, pp. 97-108, 2015, doi: 10.1016/j.apenergy.2015.04.006.

[21] H. Thanh Pham and L. Van Dai, "A Feasible MPPT Algorithm for the DC/DC Boost Converter," *International journal of electrical and computer engineering systems*, vol. 14, no. 6, pp. 713-724, 2023, doi: 10.32985/ijeces.14.6.11.

[22] S. Twaha, J. Zhu, Y. Yan, B. Li, and K. Huang, "Performance analysis of thermoelectric generator using dc-dc converter with incremental conductance based maximum power point tracking," *Energy for Sustainable Development*, vol. 37, pp. 86-98, 2017, doi: 10.1016/j.esd.2017.01.003.

[23] S. Motahhir, A. El Ghzizal, S. Sebti, and A. Derouich, "Modeling of Photovoltaic System with Modified Incremental Conductance Algorithm for Fast Changes of Irradiance," *International Journal of Photoenergy*, vol. 2018, pp. 1-13, 2018, doi: 10.1155/2018/3286479.

[24] S. Panda, S. Singh, R. Sharma, and P. R. Satpathy, "Tracking Comparison of P&O and INC Based MPPTs under Varying Weather Conditions," *2018 2nd International Conference on Data Science and Business Analytics (ICDSBA)*, pp. 198-203, 21-23 Sept. 2018 2018, doi: 10.1109/ICDSBA.2018.00042.

[25] R. Dutta and R. P. Gupta, "Performance analysis of MPPT based PV system: A case study," *2022 2nd International Conference on Emerging Frontiers in Electrical and Electronic Technologies (ICEFEET)*, pp. 1-6, 24-25 June 2022 2022, doi: 10.1109/ICEFEET51821.2022.9847729.

[26] A. Safari and S. Mekhilef, "Incremental conductance MPPT method for PV systems," *2011 24th Canadian Conference on Electrical and Computer Engineering(CCECE)*, pp. 000345-000347, 8-11 May 2011 2011, doi: 10.1109/CCECE.2011.6030470.

[27] M. Derbeli, C. Napole, and O. Barambones, "A Fuzzy Logic Control for Maximum Power Point Tracking Algorithm Validated in a Commercial PV System," *Energies*, vol. 16, no. 2, p. 748, 2023, doi: doi.org/10.3390/en16020748.

[28] K. Loukil, H. Abbes, H. Abid, M. Abid, and A. Toumi, "Design and implementation of reconfigurable MPPT fuzzy controller for photovoltaic systems," *Ain Shams Engineering Journal*, vol. 11, no. 2, pp. 319-328, 2020, doi: 10.1016/j.asej.2019.10.002.

[29] G.-I. Giurgi, L. A. Szolga, and D.-V. Giurgi, "Benefits of Fuzzy Logic on MPPT and PI Controllers in the Chain of Photovoltaic Control Systems," *Applied Sciences*, vol. 12, no. 5, p. 2318, 2022, doi: doi.org/10.3390/app12052318.

[30] P. Kumar and A. Shrivastava, "Maximum power tracking from solar PV system by using fuzzy-logic and incremental conductance techniques," *Materials Today: Proceedings*, vol. 79, pp. 267-277, 2023/01/01/ 2023, doi: doi.org/10.1016/j.matpr.2022.11.117.

[31] L. Hichem, O. Amar, and M. Leila, "Optimized ANN-fuzzy MPPT controller for a stand-alone PV system under fast-changing atmospheric conditions," *Bulletin of Electrical Engineering and Informatics*, vol. 12, no. 4, pp. 1960-1981, 2023, doi: 10.11591/eei.v12i4.5099.

[32] A. Taskin and T. Kumbasar, "An Open Source Matlab/Simulink Toolbox for Interval Type-2 Fuzzy Logic Systems," *2015 IEEE Symposium Series on Computational Intelligence*, pp. 1561-1568, 7-10 Dec. 2015 2015, doi: 10.1109/SSCI.2015.220.

[33] S. Sharma and A. J. Obaid, "Mathematical modelling, analysis and design of fuzzy logic controller for the

control of ventilation systems using MATLAB fuzzy logic toolbox," *Journal of Interdisciplinary Mathematics*, vol. 23, no. 4, pp. 843-849, 2020, doi: doi.org/10.1080/09720502.2020.1727611.